KIMIKA 16 (2) 47–51 (2000)
Printed in the Philippines

The Morphology of Palladium Nanoparticles and the Pd/Ni Bimetallic Nanocluster as Elucidated by Transmission Electron Microscopy

Myrna S. Mahinay[1]*, P. John Thomas[2], Giridhar U. Kulkarni[2], and C.N. Ramachandra Rao[2]

[1]*Chemistry Department*
Mindanao State University-Iligan Institute of Technology
Iligan City 9200, Philippines

[2]*Chemistry and Physics Material Units*
Jawaharlal Nehru Center for Advanced Scientific Research
Bangalore 560064, India

The TEM micrographs for the polymerized and thiolized palladium nanoparticle showed a well-dispersed particle with a mean particle diameter of 4.5 nm and 2.5 nm for [Pd-PVP] and [Pd-C_{12}SH] nanoparticles respectively. The bimetallic [$Pd_{0.9}$ $Ni_{0.1}$] nanocluster has a particle average diameter size of 2.75 nm for the PVP-polymerized nanocluster but has a very narrow mean particle size of 2.1 nm for the thiolized form. The notably very narrow range of particle size, uniformly dispersed particle structure of the thiolized nanocluster, and the absence of evidence of the bimodal forms in the particle structure suggest strongly an "alloying" structure of the Pd and Ni particles. This "alloying" effect will have to be further investigated using high-energy spectroscopy to affirm the said effect.

Keywords: nanoparticle; nanocluster; metal colloids; transmission electron microscopy

INTRODUCTION

In the mid 19th century, man used metal nanoparticles or colloids in ornamental decoration. The brilliant ruby-colored pigment in ruby-glass and the coloring in ceramics and chinaware were actually due to the presence of the colloidal gold particles. This fact was not readily recognized until Michael Faraday in 1857 elucidated the mechanism and preparation of stable colloidal metals that he called as divided metals [1–3]. Since then, a plethora of synthetic methods has been developed for the preparation of metal nanoparticles, colloids or sols and nanoclusters. The current enhanced interest in noble metal nanoparticles is attributed to their interesting optical, electrical, magnetic, thermal properties and their applications in microelectronics as nanoscale electronic and magnetic devices. For example, semiconductor nanoparticles such as CdS, TiO_2, ZnS, AgI and CuS, exhibit novel optical, electronic and magnetic properties due to quantum size confinement and extremely large surface-to-volume ratio relative to the bulk metal [4].

Nanoscale metal aggregates cannot be simply regarded as divided metals. Unlike the bulk metal, nanoparticles of metals do not have the conduction band but instead have the discrete states at the band edge. The confinement of the electron wavefunction at the band edge in nanoscale metal particle is allowed by the Kubo gap. The Kubo gap, δ, is the average spacing of successive quantum level and is given by the equation $\delta = 4\ E_f/3n$, where E_f is the Fermi energy of the bulk metal and n is the number of valence electrons in the nanoparticles (usually taken as the nuclearity). The Kubo gap allows the electrons to undergo quantum confinement showing the properties of a so-called quantum dots [5]. Shown in Fig. 1 is the schematic diagram of the fragmentation of a metal and the corresponding energy level diagram where the electronic continuum of the metal breaks down as the cluster size decreases. Properties such as electrical conductivity and magnetic susceptibility exhibit quantum size effect that changes the spectral features especially those related to the valence band [5]. These zero-valent metals (size ca. 1–50 nm) are usually stabilized by organic materials (ligands, surfactants, and polymers) to give redispersible metal sols [1,4].

* Author to whom correspondence should be addressed.

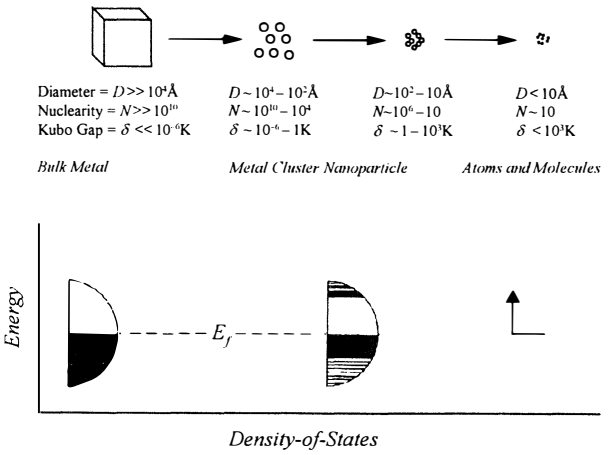

Fig. 1. Schematics of the fragmentation of a block metal and the energy diagram [1].

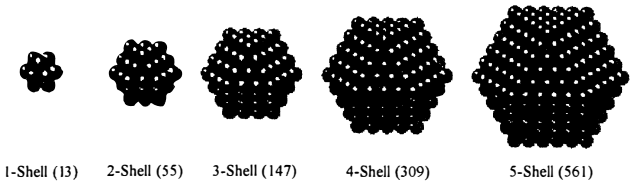

Fig. 2. Shell structure of the noble metal nanoparticle [7].

Nanoparticles have varying sizes which are well established by the magic numbers associated to nuclearity (the number of atomic shells) and electron angular momentum. The magic numbers 13, 55, 147, 309, and 561 correspond to the nuclearity of 1, 2, 3, 4, and 5 shells respectively [1]. These magic numbers are not the same magic numbers that are associated with the stability of the nuclides having closed nuclear shells in the same manner that the atomic numbers of the noble gases indicating stable electronic configurations [6]. In the case of the noble metal nanoparticles, those with the atomic shell structure shown in Fig. 2 are considered to be stable [7]. A higher proportion of the atoms in nanometal particles is present at the surface. These large portions of the surface atoms determine the size of the particle while its particle shape is determined by the crystallographic structure of the particle surface [7].

The chemical and physical properties of the nanoparticles can be determined by transmission electron microscopy (TEM) while high-resolution transmission electron microscopy (HRTEM) affords direct observation of the structures of metal nanoparticles [8]. High-energy spectroscopy can access the electronic structure of metal nanoparticles: the X-ray photoelectron spectroscopy (XPS) determines the binding energy of the level; ultraviolet photoelectron spectroscopy (UPS) and Bremmstrahling isochromat spectroscopy (BIS) provide information on the occupied and unoccupied levels near E_f; and the scanning tunneling spectroscopy (STS) provides direct information on the nonmetallic gap state [5].

This paper presents the TEM images of the palladium, Pd, and the bimetallic [$Pd_{(1-x)}Ni_x$] nanocluster prepared at the Chemistry and Physics of Material Unit, Jawaharlal Nehru Centre for Advanced Scientific Research (JNCASR), Bangalore, India.

EXPERIMENTAL

The Pd nanoparticles and [$Pd_{(1-x)}$ Ni_x] nanocluster were prepared made using the appropriate metal salts in solution phase by the chemical reduction or polyol method. Thiol-derivatization of the nanoparticles was performed with alkanethiol (C_8 SH-C_{12} SH). All the chemicals used for the synthesis of the nanosized particles were reagent grade and used as received. The polymer polyvinylpyrollidone (PVP) employed had an average molecular weight of 40,000 g mol^{-1}.

The Pd nanoparticle was prepared using 30 μmol of the 2.0 mM stock solution of H_2PdCl_4. Reduction was performed by refluxing in air for 3 h with 20% ethanol-water mixture containing a measured amount of PVP (PVP/Pd = 10). A gradual change in color from orange-yellow to brown-black marked the formation of the Pd-PVP sol. Thiol-derivatization of the Pd-PVP sol was performed by mixing thoroughly using a vortex mixer, 3.0 mL of the Pd-PVP sol, 0.4 mL of toluene and 10.0 μmL of an appropriate alkane thiol. Three mL of concentrated HCl was then added with vigorous stirring over a period of 3 min. A complete transfer of the brown-black color across the bilayer interface occurs with the colorless aqueous layer at the bottom.

The methodology used for the synthesis of the [$Pd_{(1-x)}$ Ni_x] nanocluster is similar to that reported by Miyake [7]. The bimetallic nanocluster was prepared by dissolving (1-x) mmol of palladium acetate in 1,4-dioxane for one day. This was added to a 100-ml ethylene gylcol solution of x mmol of nickel sulfate heptahydrate and 14.3 times the total mmol of metal ions of PVP (MW = 40,000 g mol^{-1}). The mixture was cooled at 5–9°C and the pH adjusted to 9–11. The whole mixture was then refluxed for 3 h over an argon atmosphere. The formation of a homogeneous brown-black sol marked the formation of [$Pd_{(1-x)}$ Ni_x] bimetallic nanocluster. Thiol-derivatization of the Pd/Ni bimetallic colloid is similar as described above for the Pd-PVP sol.

Characterizations of the Pd nanoparticle and [$Pd_{(1-x)}Ni_x$] bimetallic nanocluster were done by TEM using a JEOL-3010 Electron Microscope operating at 300 keV. A small drop of the sample was placed on a holey carbon copper grid and the solvent evaporated and further dried in vacuum for 12 h before imaging was performed.

RESULTS AND DISCUSSION

The use of TEM is indispensable for the characterization of nanocrystal materials and is very powerful for revealing the atom distribution on nanocrystal surfaces even when they are passivated with polymers. A typical TEM micrograph of the Pd nanoparticle passivated by PVP is shown in Fig. 3. The shapes of the Pd-PVP nanoparticle irrespective of the size were dispersed with a dominantly spherical structure.

The average particle size of the synthesized Pd-PVP nanoparticle is 4.5 nm (standard deviation = 0.63), being estimated from the micrograph. The distribution of the various sizes is shown in the form of a histogram alongside the TEM image. The Pd-PVP nanoparticle obtained by the above procedure using the 30 μmol of H_2PdCl_4 and 33.3 mg PVP cannot with certainty contain exactly 561 atoms in the five-shell closed configuration as Miyake *et al.* have assumed to be. Miyake *et al.* have shown that Pd nanoparticle sizes can be controlled by variation in the amount of PVP, kind and concentration of alcohol and on stepwise growth [7].

Examination of the HRTEM micrograph of the Pd-PVP nanoparticle indicated the predominance of truncated octahedral shape. The presence of other geometrical shapes such as the octahedral, prismatic, tetrahedral and twinning particles cannot be ruled out. The HRTEM image of the Pd-PVP truncated octahedral structure is shown in Fig. 4 with a model of the particle shape alongside the image.

A thiol-derivatized Pd nanoparticle was obtained as described in the experimental section. Figure 5 shows a low resolution TEM image of the thiol-derivatized Pd nanoparticles using dodecanethiol. The [Pd-C_{12}SH] nanoparticles were considerably well dispersed, and the size distribution as shown in

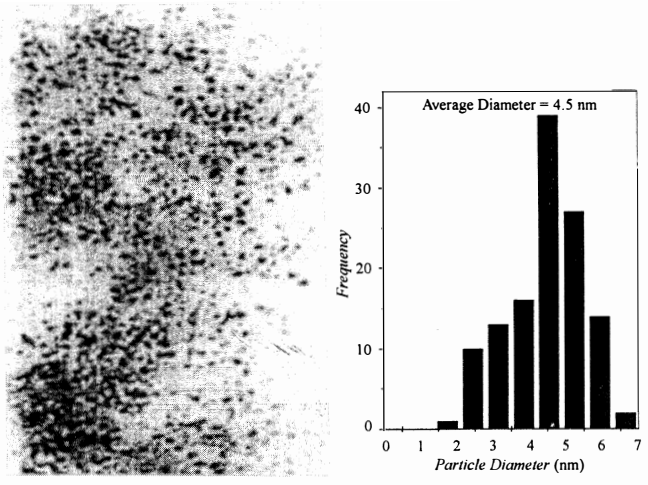

(A) (B)

Fig. 3. (A) *A low resolution TEM micrograph of colloidal Pd-PVP nanoparticle* (PVP/Pd=10; 20% ethanol); (B) *histogram showing the size distribution of the nanoparticles.*

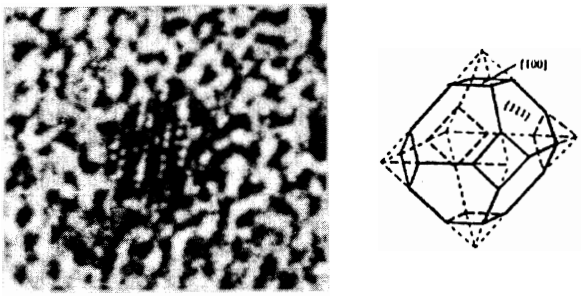

(A) (B)

Fig. 4. (A) *A high resolution TEM micrograph of the truncated octahedral structure of the Pd-PVP nanoparticle;* (B) *a model of the particle shape.*

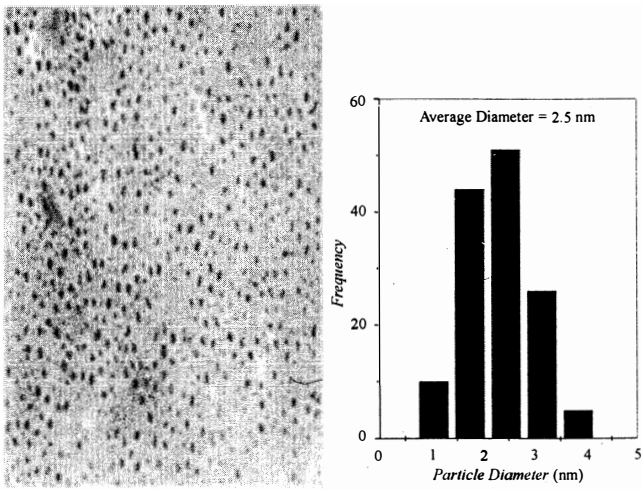

(A) (B)

Fig. 5. (A) *A low resolution TEM micrograph of the thiolized nanoparticle [Pd-C_{12}SH];* (B) *the estimated size distribution of the particle.*

the histogram is reasonably narrow relative to the polymerized [Pd-PVP] nanoparticle. The mean diameter of 2.5 nm with a standard deviation of 0.68 was estimated from the micrograph. C.N.R Rao *et al.* have obtained two-dimensional nanocrystalline arrays of the thiol-derivatized Pd nanoparticle of definite nuclearity. Shown in Fig. 6 are the TEM images of Pd_{561} and Pd_{1415} two-dimensional arrays of the thiol-derivatized Pd clusters with the lattice fringes of individual clusters shown in the inset [1].

A bimetallic nanocluster composed of Pd and Ni was also prepared. Attempts to prepare Ni noble-metal nanocluster were met with difficulties since the particles coagulated, probably due to the magnetic property of the nickel. A TEM image of the [$Pd_{0.9}$ $Ni_{0.1}$] bimetallic nanocluster is shown in Fig. 7. The average particle diameter size of 2.75 nm (std. deviation = 0.96) was obtained from the micrograph. Although the particles were well dispersed, it was difficult to elucidate with

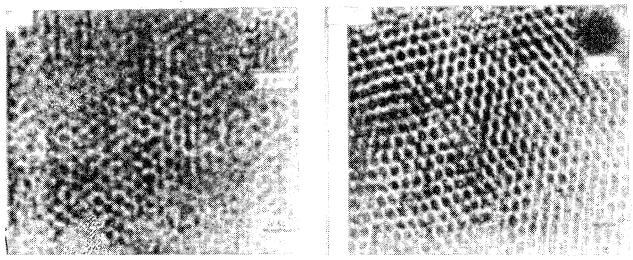

(A) (B)

Fig. 6. Two dimensional arrays of the thiolized (A) Pd_{561} *and* (B) Pd_{1415}. (Unpublished; reproduced with permission from C.N. Rao, *et al.*)

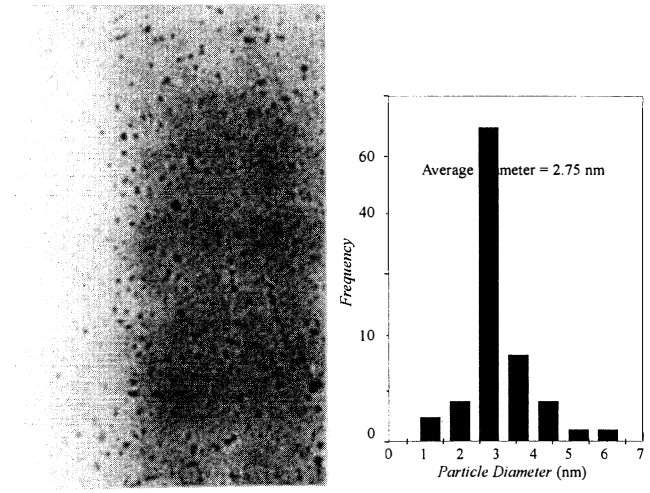

(A) (B)

Fig. 7. (A) *A low resolution TEM image of* $[Pd_{(1-x)}Ni_x]$*-PVP nanocluster;* (B) *the size distribution in histogram* (10% Ni; ethylene gylcol).

certainty from the micrograph alone an "alloy" structure. However, when the same $[Pd_{0.9}\ Ni_{0.1}]$-PVP polymerized nanocluster was thiolized with hexanethiol (C_6SH), the TEM micrograph clearly showed uniformly well dispersed particles that do not show any evidence of bimodal features. Shown in Fig. 8 is the low-resolution micrograph of the thiolized nanocluster, $[Pd_{0.9}\ Ni_{0.1}]$–C_6SH, with the histogram showing a very small particle mean diameter of 2.1 nm (std. deviation = 0.26). This notably narrow range of particle size suggests strongly an "alloying" structure involving both palladium and nickels atoms and not a mixture of the nanometallic palladium and nickel. The uniformly dispersed particle structure indicates no different growth rates that would have characterized each of the two metal nanoparticles in the absence of an "alloying" effect. The use of high-energy spectroscopy such as UPS, XPS, and STS could further enhance the characterization of the "alloying" effect on the polymerized and thiolized bimetallic nanocluster of $[Pd_{0.9}\ Ni_{0.1}]$.

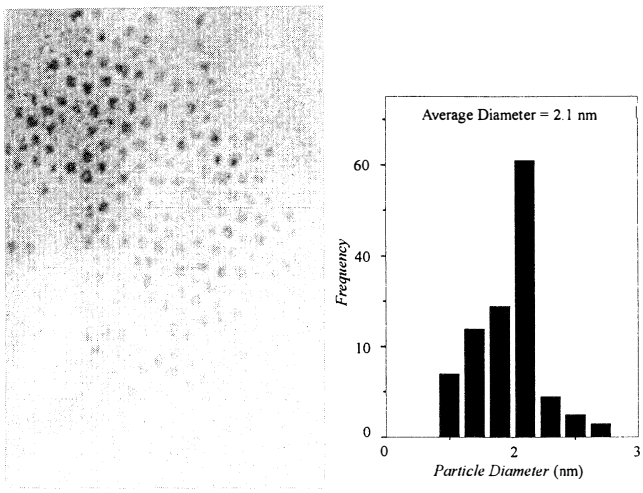

(A) (B)

Fig. 8. **(A)** ***A low resolution TEM micrograph of the thiolized*** $[Pd_{0.9}\ Ni_{0.1}]$***–*** C_6SH ***nanocluster and*** **(B)** ***the size distribution in histogram.***

CONCLUSION

The TEM images obtained for the polymerized and thiolized palladium particles showed well-dispersed particles with narrow ranges of particle diameter sizes. The results clearly show a nanoscale aggregate of the palladium particle; however, the particle size alone could not indicate with certainty the production of exactly the 561 atoms in the five-shell closed configuration or the magic number configuration of the particle. In the case of the bimetallic $[Pd_{0.9}\ Ni_{0.1}]$ nanocluster, the TEM images confirm the production of very small particles without evidence of bimodal forms in the colloidal dispersion. This can be strongly correlated to the formation of an "alloying" structure; however, further investigation using high-energy spectroscopy will confirm the "alloying" effect of the nanocluster thus obtained.

ACKNOWLEDGEMENT

This research work was supported by the Jawaharlal Nehru Centre for Advanced Scientific Research-Committee of Science and Technology for Developing Countries: International Council of Scientific Union (JNCASR-COSTED: ICSU, UNESCO), India. The author also acknowledges the support of Mindanao State University-Iligan Institute of Technology, Iligan City, Philippines.

REFERENCES

1. Ramachandra Rao, C. N., Kulkarni, G. U., Thomas, P. J., and Edwards, P. P. *Chem. Soc. Rev.* 29, 27 (2000).

2. Bonnemann, H., and Brijoux, W. *Metal Clusters in Chemistry. In* (Eds.) P. Braunstein, L.A. Oro, P.R. Raithby, Wiley-VCH, Weinheim. 2, 913 (1999).

3. Faraday, M. *Philos. Trans. R. Soc.* (London, 1857).

4. Bradley, J.S. *Clusters and Colloids: From Theory to Application.* G. Schmid, VCH, Meinheim (Ed.) Chap. 6., 459 (1994).

5. Rao, C. N. R., Kulkarni, G. U., Govindaraj, A., Satishkumar, B. C., and Thomas, P. J. *Pure and Applied Chemistry*. 72, 21 (2000).

6. Mortimer, C. E. *Chemistry: A Conceptual Approach*, 2nd ed. (Van Nostrand Reinhold Co., 1971).

7. Teranishi, T. and Miyake, M. *Chem. Mater.* 14, 594 (1998).

8. Wang, Z. L. *J. Phys. Chem B.* 104, 1153 (2000).

9. Lu, P., Teranishi, T., Asakura, K., Miyake, M., and Toshima, N. *J. Phys. Chem. B.* 103, 9673 (1999).